01 Sep 2016

Experimental and Numerical Investigations of Dust Effects on Surface Charging in Plasma

Kevin Chou

Daoru Frank Han
Missouri University of Science and Technology, handao@mst.edu

Joseph J. Wang

Recommended Citation

K. Chou et al., "Experimental and Numerical Investigations of Dust Effects on Surface Charging in Plasma," *Proceedings of the AIAA Space and Astronautics Forum and Exposition, SPACE 2016 (2016, Long Beach, CA)*, American Institute of Aeronautics and Astronautics (AIAA), Sep 2016.
The definitive version is available at https://doi.org/10.2514/6.2016-5446

AIAA SPACE Forum
13 - 16 September 2016, Long Beach, California
AIAA SPACE 2016

Experimental and Numerical Investigations of Dust Effects on Surface Charging in Plasma

Kevin Chou*
University of Southern California, Los Angeles, CA 90089-1192, USA
Daoru Han†
Worcester Polytechnic Institute, Worcester, MA 01609, USA
Joseph J. Wang‡
University of Southern California, Los Angeles, CA 90089-1192, USA

A series of 3-D, fully kinetic particle-in-cell (PIC) simulations were performed to simulate mesothermal plasma flow self-consistently with surface charging. Simulation results of plasma charging of a conducting surface covered by a thin dust layer in a plasma of cold ions and thermal electrons are presented. The surface potentials and potentials inside the dust layer are compared with experimental results. Results show that a layer of dust over a conducting surface creates a capacitance, which drives the surface more negative with respect to the ambient plasma.

I. Introduction

Spacecraft charging has been a subject of extensive investigations over the past decades,[1−5] and dust charging has been a subject of substantial studies in recent years.[6−12] However, most studies on spacecraft charging have focused on the charging of a "clean" surface in a plasma, and previous studies on dust charging have focused on the charging of single, isolated dust grains. When a spacecraft is in a dusty environment, where the inter-dust grain distances are smaller than or comparable to the plasma Debye length, such as that found near comets and certain asteroids, or on the surfaces of asteroids, the Moon, Mars, etc., its surfaces will be covered by a layer of dust particles ("dusty surface" condition), and the spacecraft surface potential becomes dependent on both the charging of the dust layer and the current balance condition. For a "dusty surface" condition, the charge of individual dust grains will be strongly affected by that of neighboring grains and the surface potential, unlike the charging of single, isolated dust grains, which is only dependent on current collection.

Ding et al.,[13] Yu et al.,[14] and Chou et al.[15] recently presented laboratory measurements of charging of a dusty surface in a mesothermal plasma. They found that charge of a dust grain on a dust layer will be one to two orders of magnitude less than that of an isolated dust grain when charged to the same potential.

In this study, a number of numerical simulation are performed to determine the charging of a surface covered by dust grains in plasma. The focus is to determine the effects on surface charging of dust grain accumulation on a conducting surface. Section II describes the numerical simulation setup. Section III presents simulation results of the plasma environment, the dust surface potential, and the potential within the dust layer and compares them with experimental results obtained in Chou et al.[15] Section IV contains a summary and conclusion.

*Graduate Research Assistant,Department of Astronautical Engineering, 854B Downey Way, Los Angeles, California 90089-1192, AIAA Student Member
†Assistant Research Professor, Aerospace Engineering Program, Mechanical Engineering Department, AIAA Member
‡Associate Professor, Department of Astronautical Engineering, 854B Downey Way, Los Angeles, California 90089-1192, AIAA Associate Fellow

Table 1. Experimentally measured plasma field parameters

	Number density n ($\times 10^7$ cm^{-3})	Drifting velocity v_d ($\times 10^6$ cm/s)	Thermal velocity v_t ($\times 10^6$ cm/s)	Temperature T (eV)	Debye length λ_D (mm)
Electrons	8.5	7.9	59.3	2	1.68
Ions	10.0	7.9	0.01	0.03	0.13

II. Numerical Simulation Setup

To determine the effects of dust accumulation on surface charging, we compared the charging of two different dust layer thicknesses (1.6 mm and 3.2 mm thick) on a 152.4 mm long conducting plate placed 177.8 mm downstream of a mesothermal plasma flow. A 3-D, fully kinetic particle-in-cell (PIC) code[16−18] was employed to simulate the plasma flow self-consistently with surface charging. Simulation particles representing both ions and electrons were included in the PIC simulations, and the plasma parameters were normalized by electron temperature and Debye length, which were determined experimentally and shown in Table 1.

The conducting plate and dust layer were modeled as an interface inside the computation domain via the immersed-finite-element (IFE) scheme (See Refs[16−18] and references therein for details). For a 1.6 mm thick dust layer (normalized to one Debye length), the domain size was 120 cells by 2 cells by 250 cells with a mesh size of 1.0 in the x- and y-direction and of 0.2 in the z-direction, for a normalized domain size of 120 $\times$ 1 $\times$ 50. The plate interface was set at z = 12.99, and the dust surface was set at z = 13.99. A mesh size of 0.2 in the z-direction was necessary to resolve the potential within the dust layer. For a dust layer of 3.2 mm (normalized thickness of two Debye lengths), the domain size was 240 cells by 2 cells by 100 cells with a mesh size of 0.5 in all directions for a normalized domain size of 120 $\times$ 1 $\times$ 50. The plate interface was set at z = 12.99, and the dust surface was set at z = 14.99.

Particles were pre-loaded into the simulation domain with a full Maxwellian distribution and drifting along the positive x-direction. At the boundaries, particles were injected at $X_{\min}$, $X_{\max}$, and $Z_{\max}$, and absorbed at $X_{\min}$, $X_{\max}$, $Z_{\min}$, and $Z_{\max}$ within each PIC iteration step. Reflection particle boundary conditions were applied at $Y_{\min}$ and $Y_{\max}$, and the potential at $Z_{\min}$ was fixed at the experimentally measured potential, listed in Table 2. The plasma species (cold, drifting ions and stationary, thermal electrons) flowed through the simulation domain for a number of simulation steps with a time step size of 0.1. The normalized velocity parameters chosen for each tests are shown in Table 3.

Table 2. Conducting plate floating potential

Dust Thickness	Floating Potential [V]
1.6 mm	-13.9
3.2 mm	-15.1

Table 3. Normalized ion and electron velocities

Species	$\hat{n}$	$\hat{v_d}$	$\hat{v_t}$	$\hat{T}$
Electrons	1.0	0.117000	1.000000	1.000000
Ions	1.0	0.117000	0.000424	0.015000

III. Results and Discussions

III.A. Plasma Field

Figure 1 compares the plasma potential, Φ_p, ion density, n_i, and electron density, n_e between the numerical simulation (left images) and experimental measurements (right images). The experimental figures shown

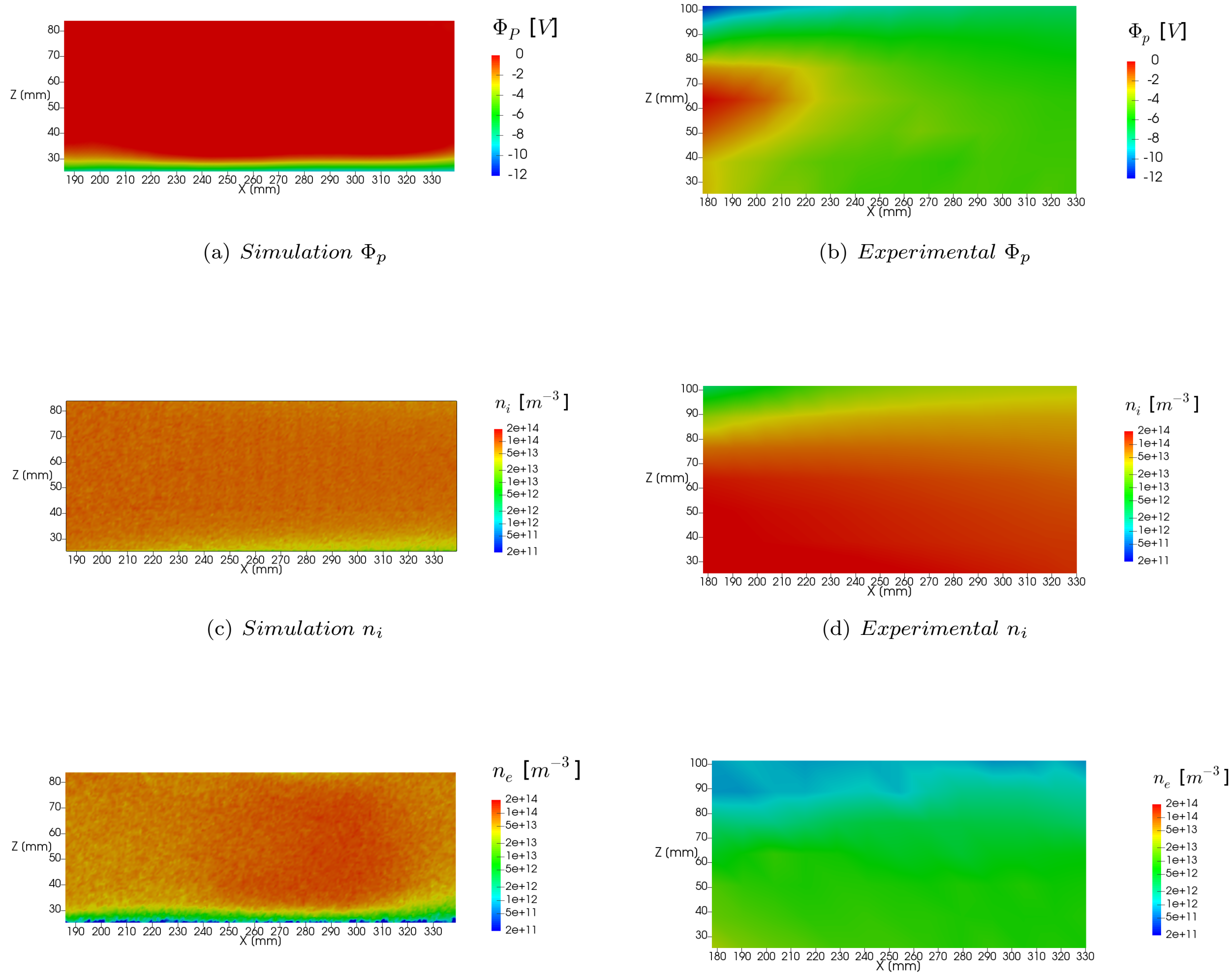

(a) *Simulation* Φ_p

(b) *Experimental* Φ_p

(c) *Simulation* n_i

(d) *Experimental* n_i

(e) *Simulation* n_e

(f) *Experimental* n_e

Figure 1. Simulation plasma environment (left) versus experimenta plasma environment (right) above the surface. The centerline of the beam is at 63.5 mm.

only contain the field 25.4 mm above the surface due to the physical limitations of the probes used to measure the laboratory beam field parameters, and so simulation fields of the same domain size are used for direct comparison. Note that the centerline of the plasma beam is 63.5 mm above the surface.

Figure 2 takes the 1-D potentials from the beam core to the sample plate at x = 228.6 mm, x = 254.0 mm, x = 279.4 mm, and x = 304.8 mm and shows that the simulation potentials are more positive than the experimentally measured potentials. This is because a uniform, quasi-neutral ambient plasma flow is used to simulate the plasma flow environment, but the laboratory plasma is non-uniform and diverges, becoming more negative downstream from beam exit. Though the beam diverges, the laboratory beam core parameters can still be used to simulate a bulk flow of mesothermal plasma above the surface because the plasma region of interest with respect to surface charging is within the sheath of the surface, and the plasma flow outside the sheath does not affect the sheath profile or surface charging at steady state.

Due to the physical constraints of the emissive probe used to measure the beam potential, the closest measurement to the surface can only be taken at 25.4 mm above the surface, so the sheath potential above the dust cannot be resolved.

III.B. Surface Charging

Figures 4 and 5 compares the experimental and simulated 1-D charging potential profiles from the surface of a 1.6 mm and 3.2 mm dust layer to the conducting plate below. The experimental data collection method can

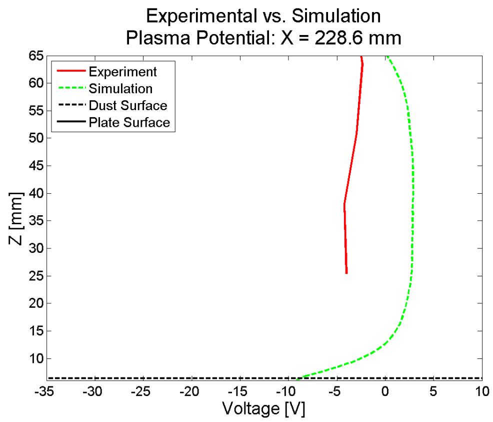

(a) $x = 228.6\ mm$

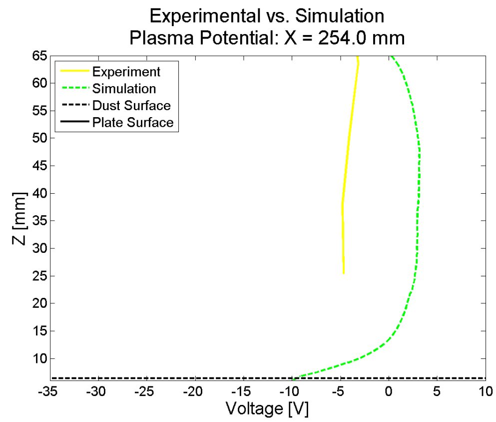

(b) $x = 254.0\ mm$

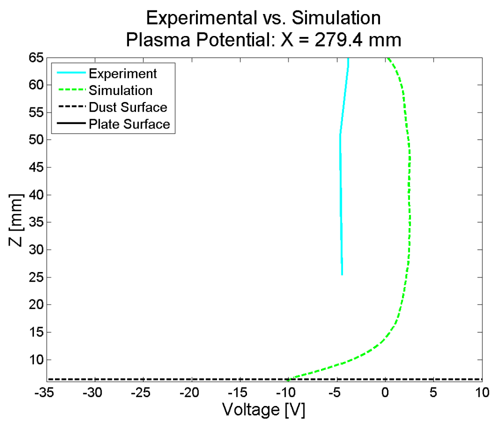

(c) $x = 279.4\ mm$

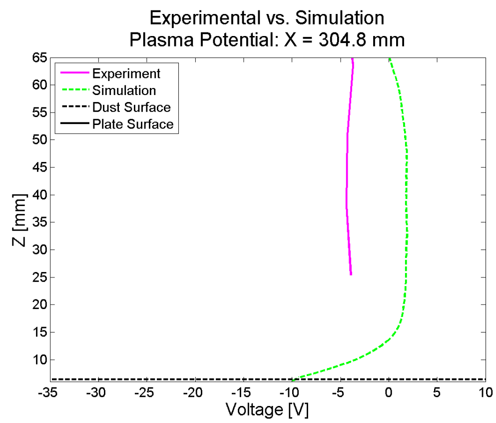

(d) $x = 304.8\ mm$

Figure 2. 1-D plasma potential profile above the sample plate at x = 228.6 mm, x = 254.0 mm, x = 279.4 mm, and x = 304.8 mm respectively.

be found in Chou et al.[15] The dust surface potential with respect to ambient potential is purely dependent on the charge deposition on the surface. The potential within the dust layer is determined by the assumption that there is no charge transport within the dust layer and can be modeled by Figure 3 and Eq. 1.

$$-(\epsilon_2 \mathbf{E_2} - \epsilon_1 \mathbf{E_1}) \cdot \mathbf{n} = -\sigma_s \tag{1}$$

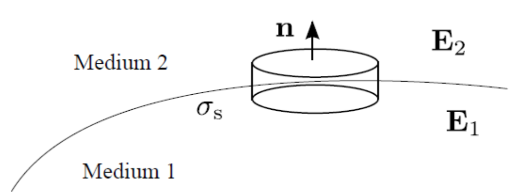

Figure 3. Flux jump across the interface caused by surface charging.

Figures 4 and 5 show that the simulation dust surface charges to the same potential regardless of dust thickness, similarly to the experimentally measured dust surface potentials shown in Table 4. Though the simulation potentials are less negative than the experimental potentials, which can again be explained by the uniform, quasi-neutral plasma flow used in the simulation, these results show that the dust surface charging is dependent only on charge deposition from the ambient plasma environment. The potential within the dust layer monotonically decreases towards the plate potential, as also seen in the experimenta results, and supports the use of embedded wires to measure the potential within a dust layer performed by Chou et al.[15]

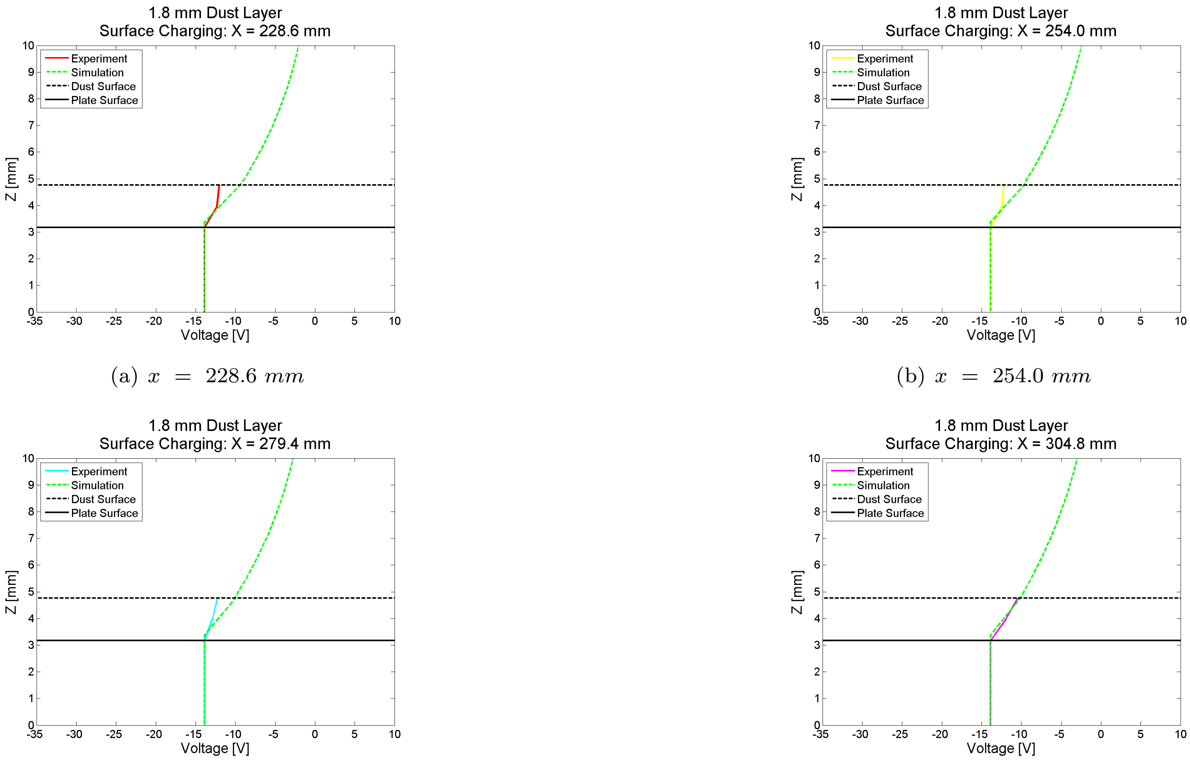

(a) $x = 228.6\ mm$ (b) $x = 254.0\ mm$

(c) $x = 279.4\ mm$ (d) $x = 304.8\ mm$

Figure 4. 1-D dust and plate potential profile from the dust surface to the plate surface at x = 228.6 mm, x = 254.0 mm, x = 279.4 mm, and 304.8 mm, respectively, for a 1.8 mm dust thickness layer.

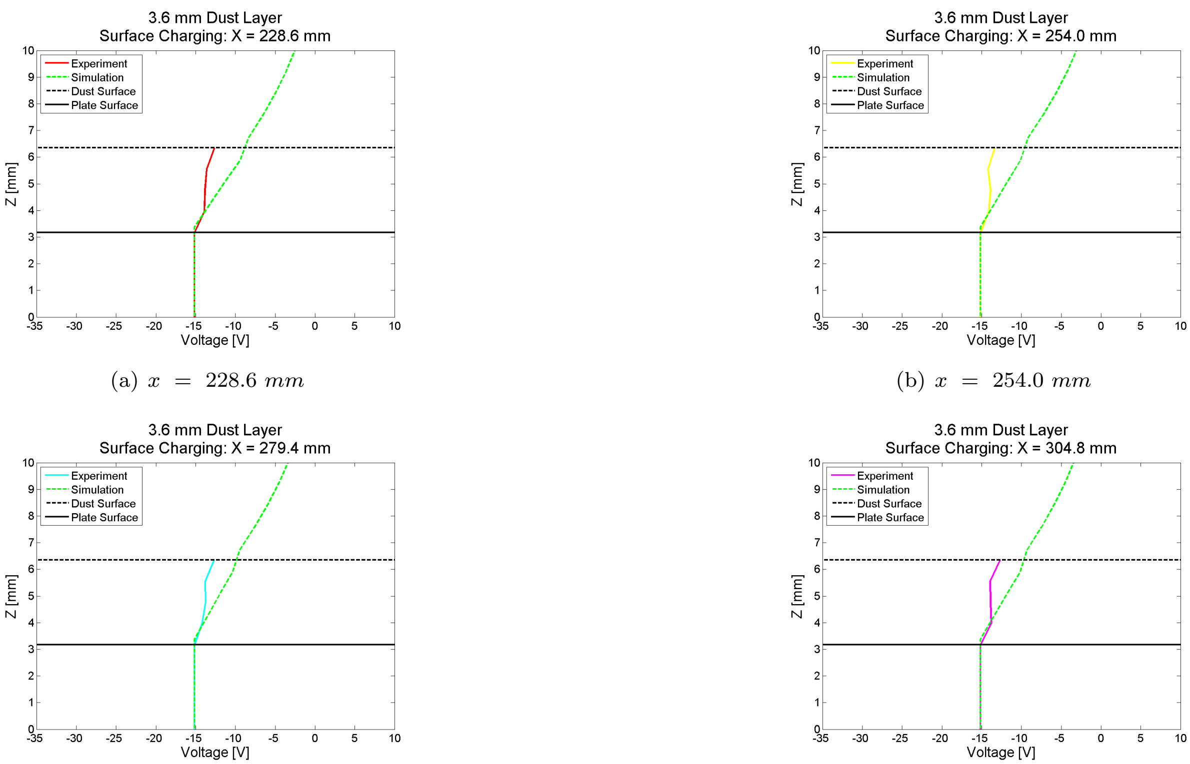

(a) $x = 228.6\ mm$ (b) $x = 254.0\ mm$

(c) $x = 279.4\ mm$ (d) $x = 304.8\ mm$

Figure 5. 1-D dust and plate potential profile from the dust surface to the plate surface at x = 228.6 mm, x = 254.0 mm, x = 279.4 mm, and 304.8 mm , respectively, for a 3.6 mm dust thickness layer.

Table 4. Experimental vs. Simulation Dust Surface Potential

Dust Thickness	Experimental [V]	Simulation [V]
1.6 mm	-11.9	-8.9
3.2 mm	-12.9	-8.9

The dust layer and conducting plate can be considered as a parallel plate capacitor, following:

$$C_{parallel} = \epsilon_0 \epsilon_{rd} A/d; Q = C(\Phi_s - \Phi_{plate}) \tag{2}$$

where ϵ_0 is the permittivity of free space, ϵ_{rd} the relative permittivity, A the overlapping area between the dust layer and aluminum plate, d the dust thickness, Φ_s the dust surface potential, and Φ_{plate} the plate potential. Using a relative permittivity of 4.29 for JSC-1A, an area of 1500 cm^2, we can calculate the capacitance for the experimental setup described in Chou et al.[15] and find the total surface charge and charge per dust grain for a 100 µm diameter grain in the simulation.

Table 5. Total charge on dust layer and charge per dust grain

Dust Thickness	*Simulation* Q_{total} $[e]$	*Experimental* Q_{total} $[e]$	*Simulation* Q_d $[e]$	*Experimental* Q_d $[e]$
1.8 mm Dust Layer	6.7×10^9	3.3×10^9	3.5×10^3	1.7×10^3
3.6 mm Dust Layer	4.5×10^9	2.4×10^9	2.3×10^3	1.3×10^3

Table 5 shows that the simulation charge per dust grain is on the same order as that found experimentally and supports the conclusion by Yu et al.[14] and Chou et al.[15] that the charge stored by an individual dust grain on a regolith surface will be significantly reduced compared to that of a single, isolated dust grain.

IV. Conclusion

A series of 3-D, fully kinetic PIC simulations were performed to understand how a dust layer charges and affects the floating potential of a conducting surface in a mesothermal plasma. We find that dust surface charging is dependent only on charge deposition from the ambient plasma and not on the dust thickness or conducting plate potential. The floating potential of a conducting plate below a dust layer is driven by dust thickness and parallel plate capacitance.

References

[1] H.B. Garrett, "The charging of spacecraft surfaces," *Reviews of Geophysics and Space Physics*, vol. 19, no. 4, pp. 577-616, 1981.

[2] E.C. Whipple,"Potentials of surfaces in space," *Reports on Progress in Physics*, vol. 44, pp. 1197-1250, 1981.

[3] H.B. Garrett and A.C. Whittlesey, "Spacecraft charging, an update," *IEEE Transactions on Plasma Science*, vol. 28, no. 6, pp. 2017-2028, 2000.

[4] D.C. Ferguson, "New frontiers in spacecraft charging," *IEEE Transactions on Plasma Science*, vol. 40, no. 2, pp. 139-143, 2012.

[5] J.C. Conger and D.E. Hastings, "Control of particle-spacecraft interactions in a LEO near-spacecraft environment," *31st Aerospace Sciences Meeting and Exhibit*, AIAA 93-0566, 1993.

[6] X. Wang, J. Colwell, M. Horányi, and S. Robertson, "Charge of dust on surfaces in plasma," *IEEE Trans. on Plasma Science*, vol. 35, no. 2, pp. 271–279, 2007.

[7] J. Goree, "Charging of particles in plasma," *Plasma Sources Science and Technology*, vol. 3, no. 3, pp. 400-406, 1994

[8] A. Barkan, N. D'Angelo, and R.L. Merlino, "Charging of dust grains in plasma," *Physical Review Letters*, vol. 73, no. 23, pp. 3093-3096, 1994

[9] M. Hornáyi, "Charged dust dynamics in the solar system," *Annual Review of Astronomy and Astrophysics*, vol. 34, pp. 383-418, 1996.

[10] X. Wang, M. Horányi, and S. Robertson, "Dust transport on a surface in plasma," *IEEE Transactions on Plasma Science*, vol. 39, no. 11, pp. 2730-2731,2011

[11] B. Walch, M. Horányi, and S. Robertson, "Electrostatic charging of lunar dust," *Physics of Dust Plasma: Seventh Workshop*, 1998

[12]M. Lampe, G. Joyce, G. Ganguli, and V. Gavrishchaka, "Interactions between dust grains in a dusty plasma," *Physics of Plasma*, vol. 7, no. 10, pp. 3851, 2000

[13]N. Ding, J. Wang, and J. Polansky, "Measurement of dust charging on a lunar regolith simulant surface," *IEEE Transactions on Plasma Science*, vol. 41, no. 12, pp. 3498-3504, 2013.

[14]W. Yu, J. Wang, and K. Chou, "Laboratory measurement of lunar regolith simulant surface charging in a localized plasma wake," *IEEE Transactions on Plasma Science*, vol. 43, no. 12, pp. 4175-4181, 2015.

[15]K. Chou, J. Wang, W. Yu, "Laboratory measurements of dust effects on surface charging in plasma," *Manuscript in preparation.*

[16]Daoru Han, "Particle-in-Cell Simulations of Plasma Interactions with Asteroidal and Lunar Surfaces," *Ph.D. Dissertation*, University of Southern California, Los Angeles, California, USA, 2015.

[17]D. Han, P. Wang, X. He, T. Lin, and J. Wang, "A 3D immersed finite element method with non-homogeneous interface flux jump for applications in particle-in-cell simulations of plasma-lunar surface interactions," *Journal Computational Physics*, vol. 321, pp. 965-980, September 2016.

[18]D. Han, J. Wang, and X. He, "A Nonhomogeneous Immersed-Finite-Element Particle-in-Cell Method for Modeling Dielectric Surface Charging in Plasmas," *IEEE Transactions on Plasma Science*, vol. 33, no. 8, pp. 1326-1332, August 2016.